
AFRL-RH-WP-TR-2012-0152

# COLORIMATETRIC DETECTION WITH APTAMER-GOLD NANOPARTICLE CONJUGATES: EFFECT OF APTAMER LENGTH ON RESPONSE

**Jorge L. Chavez, Nancy Kelley-Loughnane, Morley O. Stone**
**711 Human Performance Wing**

**Robert I. MacCuspie**
**National Institute of Standards and Technology (NIST)**
**Ceramics Division**
**100 Bureau Drive**
**Gaithersburg, MD 20899-1070**

**November 2012**
**Interim Report**



**AIR FORCE RESEARCH LABORATORY**
**711$^{TH}$ HUMAN PERFORMANCE WING,**
**HUMAN EFFECTIVENESS DIRECTORATE,**
**WRIGHT-PATTERSON AIR FORCE BASE, OH 45433**
**AIR FORCE MATERIEL COMMAND**
**UNITED STATES AIR FORCE**

## NOTICE AND SIGNATURE PAGE

Using Government drawings, specifications, or other data included in this document for any purpose other than Government procurement does not in any way obligate the U.S. Government. The fact that the Government formulated or supplied the drawings, specifications, or other data does not license the holder or any other person or corporation; or convey any rights or permission to manufacture, use, or sell any patented invention that may relate to them.

This report was cleared for public release by the 88th Air Base Wing Public Affairs Office and is available to the general public, including foreign nationals. Copies may be obtained from the Defense Technical Information Center (DTIC) (http://www.dtic.mil).

**AFRL-RH-WP-TR-2012-0152** HAS BEEN REVIEWED AND IS APPROVED FOR PUBLICATION IN ACCORDANCE WITH ASSIGNED DISTRIBUTION STATEMENT.

| | |
|---|---|
| //Signed// | //Signed// |
| Nancy Kelley-Loughnane, PhD. | Louise A. Carter, PhD. |
| Work Unit Manager | Human Centered ISR Division |
| Human Signatures Branch | Human Effectiveness Directorate |
| | 711th Human Performance Wing |
| | Air Force Research Laboratory |

This report is published in the interest of scientific and technical information exchange, and its publication does not constitute the Government's approval or disapproval of its ideas or findings.

# REPORT DOCUMENTATION PAGE

*Form Approved*
*OMB No. 0704-0188*



| 1. REPORT DATE *(DD-MM-YY)* | 2. REPORT TYPE | 3. DATES COVERED *(From - To)* |
|---|---|---|
| 30 11 12 | Interim | February 2008 – September 2011 |

**4. TITLE AND SUBTITLE**
Colorimetric Detection with Aptamer-Gold Nanoparticle Conjugates: Effect of Aptamer Length on Response

**5a. CONTRACT NUMBER**
In-House

**5b. GRANT NUMBER**

**5c. PROGRAM ELEMENT NUMBER**
62202F

**6. AUTHOR(S)**
Jorge L. Chávez[*], Robert I. MacCuspie[**], Nancy Kelley-Loughnane[*] and Morley O. Stone[*]

**5d. PROJECT NUMBER**
7184

**5e. TASK NUMBER**
D

**5f. WORK UNIT NUMBER**
H05B (7184D417)

**7. PERFORMING ORGANIZATION NAME(S) AND ADDRESS(ES)**
**National Institute of Standards and Technology
Ceramics Division
100 Bureau Drive
Gaithersburg, MD 20899

**8. PERFORMING ORGANIZATION REPORT NUMBER**

**9. SPONSORING/MONITORING AGENCY NAME(S) AND ADDRESS(ES)**
*Air Force Materiel Command
Air Force Research Laboratory
711th Human Performance Wing
Human Effectiveness Directorate
Human Centered ISR Division
Human Signatures Branch
Wright-Patterson Air Force Base, OH 45433

**10. SPONSORING/MONITORING AGENCY ACRONYM(S)**
711 HPW/RHXB

**11. SPONSORING/MONITORING AGENCY REPORT NUMBER(S)**
**AFRL-RH-WP-TR-2012-0152**

**12. DISTRIBUTION/AVAILABILITY STATEMENT**
Distribution A: Approved for public release; distribution is unlimited

**13. SUPPLEMENTARY NOTES**
88ABW-2011-6451, cleared 15 Dec 11

**14. ABSTRACT**
A riboflavin binding aptamer (RBA) was used in combination with gold nanoparticles (AuNPs) to detect riboflavin *in vitro*. The RBA-AuNPs responded colorimetrically to the presence of riboflavin and this response could be followed by the naked eye. We used this system as a model to study how modifications on the aptamer sequence affect the response of the aptamer-AuNP conjugates (Apt-AuNPs) to their target. To mimic primers and other sequence modifications typically used in aptamer work, the RBA was extended by adding random bases to its 5' end and the response of these Apt-AuNPs was evaluated. These extra bases were designed to avoid interactions with the RBA binding site. We observed that the length of the aptamer significantly affected the Apt-AuNPs stability and the magnitude of the detection response to riboflavin. The addition of thymine nucleotides instead of random tails to the RBA showed that the effects observed were not specific to the sequence used but rather general. This work shows that modifications of the aptamer sequence provide a means to improve the Apt-AuNPs sensing response.

**15. SUBJECT TERMS**
riboflavin binding aptamer, gold nanoparticles, aptamer-AuNP conjugates

| 16. SECURITY CLASSIFICATION OF: | | | 17. LIMITATION OF ABSTRACT: | 18. NUMBER OF PAGES | 19a. NAME OF RESPONSIBLE PERSON (Monitor) |
|---|---|---|---|---|---|
| a. REPORT | b. ABSTRACT | c. THIS PAGE | | | Nancy Kelley-Loughnane |
| U | U | U | SAR | 24 | 19b. TELEPHONE NUMBER *(Include Area Code)* N/A |

**Standard Form 298 (Rev. 8-98)**
Prescribed by ANSI Std. Z39-18

**THIS PAGE IS INTENTIONALLY LEFT BLANK.**

# Colorimetric Detection with Aptamer-Gold Nanoparticle Conjugates: Effect of Aptamer Length on Response

*Jorge L. Chávez[1], Robert I. MacCuspie[2], Nancy Kelley-Loughnane[1] and Morley O. Stone[1] **

[1] 711th Human Performance Wing, Human Effectiveness Directorate, Air Force Research Laboratory, Wright-Patterson Air Force Base, OH 45433, USA

[2] Ceramics Division, National Institute of Standards and Technology, Gaithersburg, MD 20899 USA

Nancy.Kelley-Loughnane@wpafb.af.mil

ABSTRACT. A riboflavin binding aptamer (RBA) was used in combination with gold nanoparticles (AuNPs) to detect riboflavin *in vitro*. The RBA-AuNPs responded colorimetrically to the presence of riboflavin and this response could be followed by the naked eye. We used this system as a model to study how modifications on the aptamer sequence affect the response of the aptamer-AuNP conjugates (Apt-AuNPs) to their target. To mimic primers and other sequence modifications typically used in aptamer work, the RBA was extended by adding random bases to its 5' end and the response of these Apt-AuNPs was evaluated. These extra bases were designed to avoid interactions with the RBA binding site. We observed that the length of the aptamer significantly affected the Apt-AuNPs stability and the

magnitude of the detection response to riboflavin. The addition of thymine nucleotides instead of random tails to the RBA showed that the effects observed were not specific to the sequence used but rather general. This work shows that modifications of the aptamer sequence provide a means to improve the Apt-AuNPs sensing response.

INTRODUCTION. Gold nanoparticles (AuNPs) have attracted a great deal of attention as reporter units in different sensing applications due to their optical properties.[1,2,3] The color of an AuNP suspension is greatly affected by the particle stability and interparticle distance; well-dispersed AuNPs give red suspensions, while their aggregation produces a purple-blue color.[4.5] AuNP-based sensing strategies are designed by promoting a change in the AuNPs stability and aggregation state as a result of the presence of the target of interest, which produces a colorimetric response.[6] It has been demonstrated that when an aptamer is used in combination with AuNPs, the nanoparticle stability can be affected by the aptamer conformational change produced by binding the target.[7] Different strategies to combine AuNPs and aptamers (Apt-AuNPs) have been proposed, including using aptamers as reversible crosslinkers to create "sensing aggregates"[8,9] and sandwich assays for electrochemical detection.[10,11] In the last few years, more simple assays have been designed in order to obtain faster responses and minimize the manipulation and modifications of the aptamers and AuNPs. For instance, immobilizing thiol-modified aptamers on AuNPs produced Apt-AuNPs stabilized by the negative charges of the DNA. Exposing the Apt-AuNPs to the target increased the stability of the particles due to the change in conformation of the aptamer on the AuNPs surface.[12,13] In a different approach, the higher affinity of AuNPs for single-stranded DNA (ssDNA) over double stranded-DNA (dsDNA) has been used to design sensors.[14] Non-modified aptamers adsorbed on the surface of AuNPs due to their flexible conformation when the target is not present. Aptamer binding to its target occurs by adoption of a conformation that involved extensive base-pairing, resembling dsDNA. This more rigid conformation prevented the aptamer adsorption on the AuNPs, decreasing their stability.[6, 15, 7]

Aptamers have been proposed as recognition elements in different sensing strategies due to their superior stability compared to antibodies and their high affinity and selectivity for their targets.[3] Aptamer selection is typically performed in solution by the Systematic Evolution of Ligands by Exponential Enrichment (SELEX), using a random pool of oligonucleotides of a fixed length.[16,17] The selected sequences can be further optimized by different means, including removing certain bases from the binding or non-binding regions of the sequence,[18] mutations to the binding site,[19] removal of certain structural features like stems or loops,[20] etc. These optimizations are typically performed during the selection process *prior* to their use as a sensing element. There are only a few reports of work trying to understand how modifying the aptamer sequence affects the response of an aptamer when used in combination with AuNPs.[9,21] Recently, it has been shown that incorporation of aptamers selected in solution into applications which require the oligonucleotide be immobilized on a surface can prevent the aptamer activity.[22] The conformational requirements for aptamer binding to its target, which is necessary in nanoparticle-based sensing, could be completely prevented when the oligonucleotide is immobilized on a surface. Therefore, it is necessary to better understand how different parameters affect the aptamer performance in nanoparticle-based detection to design better sensing strategies.

A great amount of work has been performed to study the interactions between DNA and AuNPs in the context of DNA hybridization.[23,24] It has been shown that thymines and poly(thymine) chains interact minimally with the surface of AuNPs, contrary to the case of adenine and poly(adenine) chains.[25, 26] Other studies have shown that nonspecific interactions play an important role on the AuNP coating density when thiol-modified oligonucleotides are chemisorbed on their surfaces.[27] However, only a few reports have addressed these issues in the context of Apt-AuNPs colorimetric detection.[12,13]

In this work, we designed a simple set of experiments aimed to investigate whether modifications of an aptamer sequence affect the response of Apt-AuNPs to their target. We chose the riboflavin binding aptamer (RBA) since it has been fully characterized,[28] and has been recently used in our group as recognition element in a biofunctionalized FET device.[29] However, it has not yet been utilized with

AuNPs. A simple colorimetric detection assay for riboflavin was designed. An efficient response to the target was observed. We modified the RBA sequence by adding extra bases to the 5'end and evaluated the response of the different RBA-AuNPs obtained to riboflavin.

Experimental. *Chemicals*: All oligonucleotides were obtained from IDT (Coralville, IA) and purified by standard desalting. Riboflavin, hydrogen tetrachloroaurate(III) ($HAuCl_4$), sodium citrate, sodium chloride, Hepes, magnesium chloride and QCA were obtained from Sigma-Aldrich (St. Louis, MO). The Quant-It™ OligoGreen ssDNA reagent kit was obtained from Molecular Probes (Eugene, OR)

*AuNPs Synthesis and Characterization:* The gold nanoparticles were synthesized as reported elsewhere with slight modifications.[30] Briefly, 98 mL of Millipore $H_2O$ were mixed with 2 mL of 50 mM $HAuCl_4$ in a round bottom flask connected to a water-cooled condenser. The mixture was heated up to boiling in a silicon oil bath. As soon a reflux started, 10 mL of a 38.8 mM sodium citrate solution was added. The solution turned red after a few minutes. The reaction was allowed to continue for 20 minutes under constant stirring and heat. After cooling down, the solution was filtered with a 0.2 μm polyester membrane. The AuNPs suspensions were kept in a dark amber bottle. The AuNPs size was determined to be ~17 nm by DLS. The extinction maximum was determined to be 520 nm in a Cary 300 UV spectrophotometer (Agilent Technologies, Santa Clara, CA). The AuNP concentration was calculated to be ~ 10 nM, based on a molar absorption coefficient of $2.4 \times 10^8$ L/(mol*cm).[30]

*Preparation of Apt-AuNPs:* AuNPs (7.5 mL approx. 10 nM, "as is" after synthesis) were mixed with 45 μL of 100 μM RBA aptamer (dissolved in DNase-free water). The mixture was briefly vortexed and left in the dark without stirring for at least 5 h. This ratio gives a nominal aptamer loading of 60 aptamer units per AuNP. Subsequently, a volume of the Apt-AuNPs was mixed with an equal volume of buffer containing 20 mM Hepes, 2 mM $MgCl_2$, pH 7.4. Before the detection assay was performed, the mixture was further diluted with an equal volume of buffer containing 10 mM Hepes, 1 mM $MgCl_2$, pH 7.4. The final AuNP concentration was ~ 2.5 nM. The RBA-AuNPs were used in the colorimetric assay within two days after buffer addition.

*Riboflavin Detection:* The AuNPs were mixed with an appropriate volume of a riboflavin stock solution to obtain different riboflavin concentrations in a total volume of 200 µL. The mixtures were incubated for 10 min in a 96 well plate, protected from light. Subsequently, a volume of a 2M NaCl solution was added simultaneously to all the wells used in an experiment to obtain the same final salt concentration. After briefly mixing the samples, the plate was immediately transferred to a Spectra Max M5 plate reader (Molecular Devices, Sunnyvale, CA) and the extinction of the AuNP suspensions at 530 nm and 650 nm was monitored over time. A similar procedure was followed with the negative control, using QCA instead of riboflavin. The degree of aggregation was plotted as the ratio of the extinction intensity of the aggregated AuNPs (extinction at 650 nm) over the individual AuNPs (extinction at 530nm) as a function of target concentration.

*Dynamic Light Scattering Size Analysis*: The DLS methodology followed recommendations outlined in the NIST-Nanotechnology Characterization Laboratory (NIST-NCL) Assay Cascade protocol PCC-1[31]. Sample preparation was performed in a biosafety level 2 hood to prevent introduction of dust or other contaminants. Disposable semi-micro cuvettes and caps (BrandTech, Inc.,) were cleaned with distilled water and dried with filtered compressed air immediately before use. DLS measurements were performed using a Malvern Instruments (Westborough, MA, USA) Zetasizer Nano in 173º backscatter mode with the instrument's temperature controller set at 20.0 ± 0.1 ºC. The intensity-based size distribution was used to obtain the graph in Figure 5, considering the individual aptamer-coated particles as the species with $20 < d < 50$ nm and the aggregated particles as the scatterers with $d > 100$ nm. The samples were all studied in the same buffer: 12.5 mM Hepes, 1.25 mM $MgCl_2$. Throughout this paper, the mean of five consecutive measurements are reported with uncertainty of one standard deviation about the mean; this represents the repeatability of the measurements, and not the width of the size distribution. See Table S-I for detail size distribution data.

*Determination of Aptamer Surface Coverage on the AuNPs*. The Quant-It™ OligoGreen ssDNA reagent kit was used to determine the amount of DNA free in solution after adsorption of the aptamers

on the AuNPs. A calibration curve of the dye response was obtained for each of the five variations of the RBA used, following the manufacturer instructions. To determine the aptamer coverage, the Apt-AuNPs (500 μL) were centrifuged using Amicom filters with a MWCO of 50 KDa (Fisher Scientific, Pittsburgh, PA). The Apt-AuNPs were collected on the membrane and the clear liquid that passed through the membrane was used to determine the amount of free DNA (not adsorbed on the AuNPs.) The fluorescence intensity of each sample was measured and fit into the calibration curve to obtain the DNA concentration. The measurements were performed in duplicate.

RESULTS AND DISCUSSION. The goal of this work was to examine the effect of modifications on the aptamer sequence on the response of Apt-AuNPs to their target. A colorimetric assay was developed as shown in Scheme 1. The RBA-AuNPs were prepared by simply adsorbing the aptamer on the AuNPs (17 nm hydrodynamic diameter) at a ratio of 60 aptamer molecules per AuNP. The single stranded-flexible RBA was adsorbed on the AuNPs surface with the nitrogen bases interacting with the surface and the negative charges facing the solvent, stabilizing the AuNPs.[14] The system involves an equilibrium between aptamer molecules adsorbed on the AuNPs and free in solution.[7] Exposing the RBA-AuNPs to high ionic strength media, induced their aggregation. The sensing protocol was designed by finding the conditions of minimal NaCl concentration necessary to promote the RBA-AuNPs aggregation in the absence of the target (Scheme 1A). Our preliminary results showed that when the experiments were performed under the same conditions in the presence of riboflavin, the RBA-AuNPs did not precipitate, as shown schematically in Scheme 1B. These results indicated that the system's stability improved as a consequence of the conformation adopted by the aptamer during binding the target.

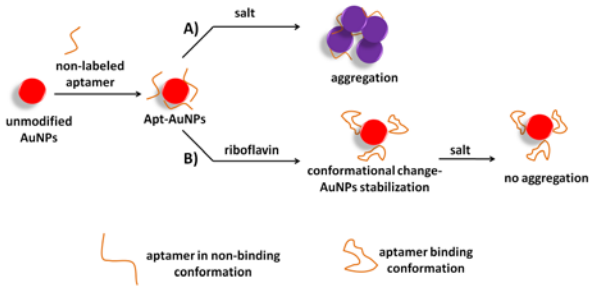


To simplify the system studied here, we used unmodified AuNPs and aptamers with no additional functional groups for immobilization. This was intended to prevent unwanted interactions between certain labeling or anchoring groups, such as thiols or biotin, with the oligos or AuNPs. To mimic aptamer modifications in the non-binding parts of the aptamer sequence, we modified the RBA by preparing two longer versions of the aptamer, see Table I for sequences. The NoTail-RBA contained only nucleotides that form the stem and the G-quartet which interacts with the target.[28] The ShortTail-RBA was obtained by adding five extra random nucleotides to the 5' end of the NoTail-RBA, while LongTail-RBA was obtained by adding seventeen extra random nucleotides. Analysis of the secondary structure of the modified versions of the aptamer by mfold[32] confirmed that the binding site was not affected by the addition of these extra nucleotides (Figure S-1). The response of the three different RBA-AuNPs obtained with the different RBAs were evaluated and compared. To investigate if the results observed were specific to the sequences used to extend the RBA, two more oligos were designed by using poly(thymine) tails (polyT). Five thymines were added to the RBA (T5-RBA) to mimic the ShortTail system and seventeen thymines were added (T17-RBA) to compare to the LongTail system, see Table I for sequences used. The polyT-RBA-AuNPs were tested in a similar way to the RBA-AuNPs obtained with the random tails.

| *Aptamer Name* | *Sequence* |
|---|---|
| NoTail | 5’ GGAACGACGGTGGTGGAGGAGATCGTTCC 3’ |
| ShortTail | 5’ AGAGAGGAACGACGGTGGTGGAGGAGATCGTTCC 3’ |
| LongTail | 5’ACTCATCTGTGAAGAGAGGAACGACGGTGGTGGAGGAGATCGTTCC 3’ |
| T5 | 5’ TTTTTGGAACGACGGTGGTGGAGGAGATCGTTCC 3’ |
| T17 | 5’ TTTTTTTTTTTTTTTTTGGAACGACGGTGGTGGAGGAGATCGTTCC 3’ |

Figure 1A shows the typical response of the RBA-AuNPs in the presence of riboflavin. The scans show the spectra of an RBA-AuNP suspension exposed to increasing concentrations of the target followed by NaCl addition. In the absence of riboflavin (black line), a shoulder at above 600 nm is observed after salt addition due to the aggregation of the RBA-AuNPs. This aggregation is due to the increase in ionic strength upon addition of NaCl.[6] When the same RBA-AuNP suspension was exposed to riboflavin prior to NaCl addition, the intensity of the aggregation peak decreased under the same conditions. Importantly, the degree of reduction of this peak was correlated to the concentration of riboflavin present. Figure 1B shows the quantification of the response of the ShortTail-RBA-AuNPs to riboflavin (red line) and to QCA (blue line), see Figure 1B for chemical structures. QCA was used during the original aptamer selection as a counter-SELEX step,[28] meaning that the selection was designed to obtain an aptamer that can bind riboflavin but not QCA. Based on this, we used QCA as a negative control, to test the ability of the aptamer to differentiate between these two molecules in this nanoparticle-based sensing system. The RBA-AuNPs degree of aggregation was quantified by using the ratio of the peak produced by the aggregated RBA-AuNPs (extinction at 650 nm-$E_{650}$) and the peak corresponding to the dispersed RBA-AuNPs (extinction at 530nm-$E_{530}$).[6] Figure 1B shows the response of the system to riboflavin and the lack of response to QCA. It is clearly observed that the presence of riboflavin prevented the AuNPs from aggregating, and that this increase in stability improved with higher concentrations of the target.

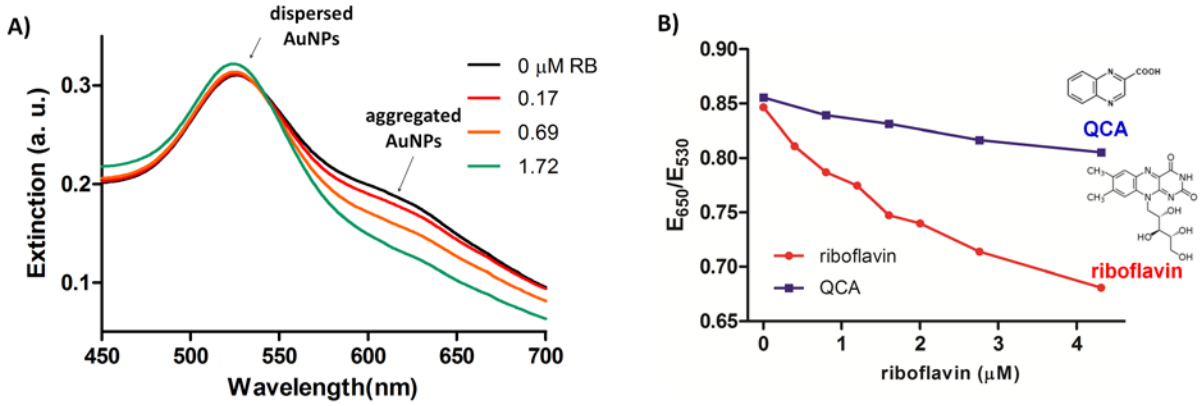


The first step in optimizing the sensing assay involved adjusting different parameters that affect the RBA-AuNPs response. Preliminary results showed that this response was affected by the ionic strength used in the aggregation step. The same trend was observed for the different systems studied here. For simplicity, we will discuss the results for the ShortTail-AuNPs. Figure S-2 shows the response of the ShortTail-RBA-AuNPs to the same riboflavin concentration range after incubation at two different NaCl concentrations. As expected, higher salt concentrations produced a larger degree of aggregation (higher $E_{650}/E_{530}$), after incubation with NaCl for three minutes. Interestingly, the RBA-AuNPs sensitivity improved when the assay was performed in higher ionic strength media. Comparison of Figures S-2A and S-2B showed that the system responded to 400 nM riboflavin at 345 mM NaCl. When 327 mM NaCl was used to challenge the ShortTail-RBA-AuNPs, the target concentration had to be increased to 800 nM to observe a response.

The length of the aptamer was observed to affect the response of the RNA-AuNPs as well. For simplicity, we will compare the aggregation response of the ShortTail-RBA-AuNPs and LongTail-RBA-AuNPs after incubation with 345 mM NaCl. The ShortTail-RBA-AuNPs aggregated more when tested under the exact same conditions as the LongTail-RBA-AuNPs (higher $E_{650}/E_{530}$), as shown in Figure S-3. The $E_{650}/E_{530}$ was approx 0.5 for the ShortTail-Apt-AuNPs when no riboflavin was present, while the LongTail-Apt-AuNP was approx 0.82, under the same conditions. Importantly, as shown in Figure S4, the aptamer loading on the AuNPs was determined to be relatively constant for all the formulations used

in this study. Only approximately 20 % (+/- 3 %) of the DNA loaded on the AuNPs was recovered in the supernatant, which gives an average coating density of ~48 aptamer molecules per AuNP, consistent with previous reports.[33] No significant difference in particle diameter before and after adsorption of the DNA was observed by DLS, which suggested that the aptamer mostly adopts a flat conformation when adsorbed on the AuNPs surface. Having a comparable number of oligos per particle on each of the systems studied means that the total particle area covered in the LongTail-RBA-AuNPs is higher than in the other RBA-AuNPs, since each LongTail-RBA unit has 17 extra bases than the NoTail-RBA and 12 extra bases than the ShortTail-RBA. Based on this, a significant difference in the stabilities of the RBA-AuNPs is expected, as observed in Figure S3.

The results discussed so far, confirmed that the aggregation state of the RBA-AuNPs affected their response. In order to perform a legitimate comparison of the response of each RBA-AuNP system to riboflavin, the NaCl concentration used was adjusted to produce a similar degree of aggregation in the absence of riboflavin. Our preliminary data showed that NaCl concentrations that produce an $E_{650}/E_{530}$ of approx 0.8 three minutes after salt addition, offered an optimal response for the colorimetric detection of riboflavin. Based on this, the response of the different RBA-AuNPs were tested under optimal buffer conditions: the NoTail- and ShortTail-RBA-AuNPs were used in 12.5 mM Hepes buffer containing 1.25 mM $MgCl_2$, while the LongTail-RBA-AuNPs was used in buffer containing 8.3 mM Hepes, 1 mM $MgCl_2$. Figure 2A shows the quantification of the responses of the three systems at different riboflavin concentrations. The ShortTail-RBA-AuNPs showed the most modest response to riboflavin. However, as shown in Figure 1B, this response is significantly better than the one for the negative control (QCA), which confirmed that the system responded selectively to the aptamer target. As shown in Figure 2A, the LongTail-RBA-AuNPs (green line) showed a more efficient response to riboflavin than the ShortTail-RBA-AuNPs (blue line). The LongTail system showed a larger difference in aggregation state ($\Delta E_{650}/E_{530}$) between the absence of target (0 μM riboflavin) and increasing riboflavin concentrations. As discussed before, the stabilization effect produced by riboflavin was correlated with its concentration

and a steady reduction on the RBA-AuNPs aggregation state (increase in stability) was observed with larger riboflavin concentrations ($\Delta E_{650}/E_{530}$ from 0 to 4.3 µM ~ 0.1 for ShortTail and ~0.4 for LongTail). The NoTail-RBA-AuNPs showed a larger stabilization effect with lower riboflavin concentrations, being able to detect as low as 100 nM riboflavin. Figure 2B shows a digital picture of the NoTail-RBA-AuNPs colorimetric response to riboflavin and QCA, showing that riboflavin monitoring can be performed with the naked eye.

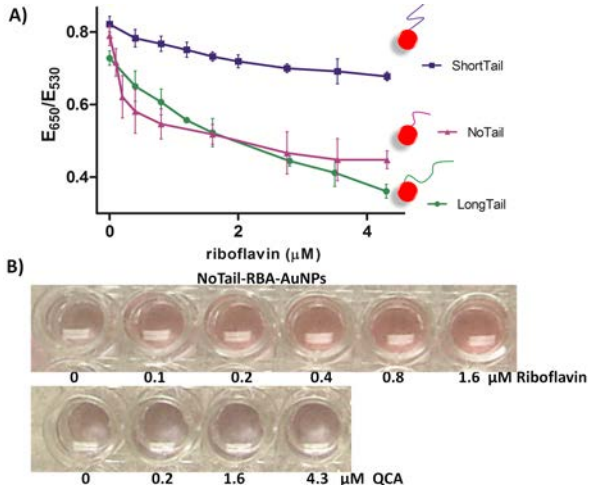


In general, the RBA-AuNPs response to riboflavin suggested that the aptamer retained its ability to bind its target without responding to QCA. Moreover, this binding was efficiently transduced by the AuNPs to a colorimetric signal. However, the response was affected by the RBA used, but was not directly correlated with the aptamer length. To better understand these observations we monitored the aggregation kinetics for each system by following changes in their extinction spectra, as shown in Figure 3. The RBA-AuNPs were used under the same conditions as shown in Figure 2 and the changes in their aggregation state were monitored for ten minutes. The aggregation kinetics data of the ShortTail-RBA-AuNPs, which showed the poorest response to riboflavin, looked dramatically different than the other two RBA-AuNPs. The ShortTail-RBA-AuNPs precipitated 8 minutes after salt addition (Figure 3B). It can be observed that the aggregation rate (the slope of the kinetic data in Figure 3B) increased at larger riboflavin concentrations. Contrary to the ShortTail-RBA-AuNP, the other two RBA-AuNPs showed a steady aggregation increase over a 10 minute period for each riboflavin concentration, and more

importantly, the systems did not precipitate. These data indicated that the intrinsic stability of the ShortTail-RBA-AuNPs is poorer than the NoTail- and LongTail- RBA-AuNPs. This may explain the poorer response of ShortTail system to riboflavin. The ShortTail-RBA-AuNPs higher tendency to precipitate after increasing the ionic strength of the media seemed to mask part of the stability enhancement produced by the RBA conformational change promoted by the binding of riboflavin.

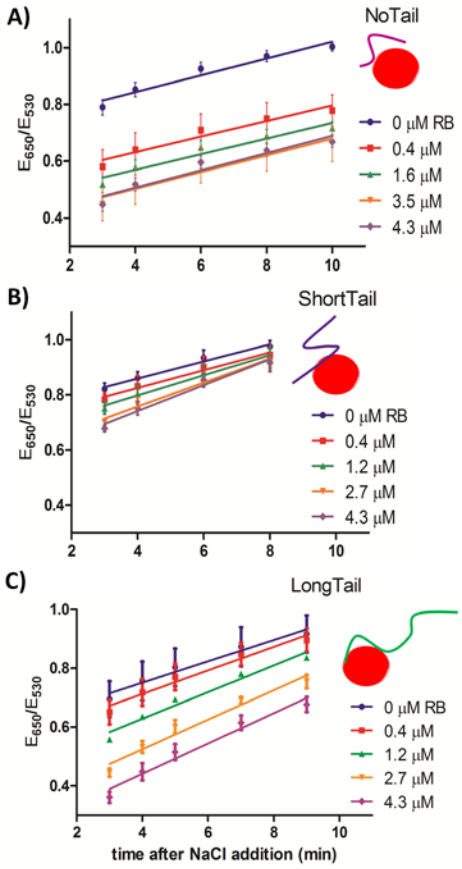


To further investigate the stability of the Apt-AuNPs used to sense riboflavin, we decided to monitor the particle size distribution at different stages of the assay protocol by DLS. Monitoring nanoparticle aggregation by DLS is a challenging task, due to the fact that the intensity of the light scattered by a particle is proportional to the sixth power of its diameter.[34] Based on this, the signal generated by nanoparticle aggregates can easily mask the presence of individual particles. To simplify the data analysis, we studied the nanoparticle size distribution *prior* to the addition of NaCl, to minimize the formation of aggregates, as shown in Figure 4. Figure 4A shows the size distribution of the three

AuNPs systems after overnight incubation with the aptamers in water. Mainly well-dispersed, individual AuNPs were present. After incubation in buffer for a few hours, the intensity-based distribution was dominated by the signal generated by the formation of agglomerates.[35] At the same time, the distribution showed a significant reduction of the dispersed AuNPs signal, although the suspensions showed no significant change in color. This can be understood, as discussed above, based on the dependence of the intensity of the scattered light on particle size. Even in cases of minor aggregation, the larger nanoparticle aggregates can mask the single particle signal. Interestingly, addition of riboflavin produced significant changes in the size distribution on the Apt-AuNPs, increasing the intensity of the single-particle signal. This data suggested that the binding of riboflavin, and the aptamer conformational change, improved the Apt-AuNPs stability in buffer, breaking the agglomerates that have formed due to the addition of buffer. Interestingly, the average RBA-AuNPs stability matched the results observed by the aggregation kinetics monitored by UV-vis spectroscopy and the colorimetric response of the Apt-AuNPs at different concentrations of riboflavin. The ShortTail-Apt-AuNPs aggregated the most after buffer addition, and despite showing an increase in the single-particle signal (6.5 to 13 %), a higher degree of aggregation compared to the other Apt-AuNPs was observed in the presence of riboflavin, see Table S-1 for a table with the DLS data. This was the system with the most modest colorimetric response to the target. On the contrary, the NoTail-Apt-AuNPs showed the most significant increase in the single-particle signal after exposure to riboflavin (25.5 to 55 %) and the best colorimetric response to the target. Following the trend in the colorimetric response, the LongTail-RBA-AuNPs showed an intermediate increase in the single-particle signal (14 to 20 %) after addition of riboflavin.

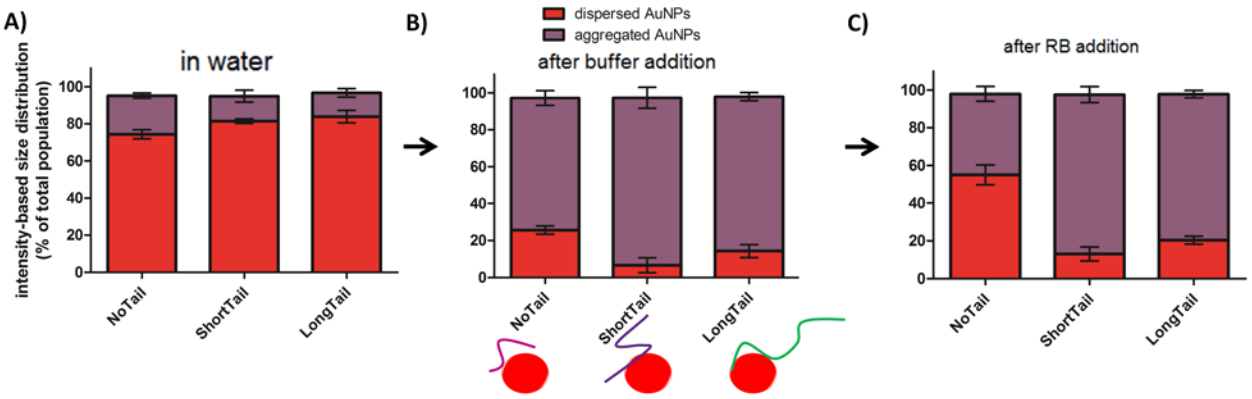


The data presented here confirmed that the response of the Apt-AuNPs to riboflavin is largely dominated by the stability of the Apt-AuNPs and, more importantly, this stability is affected by the length of the aptamer used. It is interesting to point out that the modifications in the aptamer length did not affect the secondary structure of the binding site, as predicted by mfold (Figure S-1). Although it may be possible that the tertiary structure of the aptamer is affected by such changes. To investigate whether the effects reported were specific to the random sequences used in the extra nucleotides added to the RBA, two more variations of the aptamer were designed. In these cases, a poly(thymine) was added to the 5' end of the RBA (see Table I for aptamer sequences). The polyT-RBA-AuNPs showed the same trend as the RBA-AuNPs with random tails, with the T17-RBA-AuNPs showing a better response to riboflavin than the T5-RBA-AuNPs (Figure 5A). Figure 5B shows the digital image of the T17-RBA-AuNPs response to riboflavin, which demonstrated that riboflavin monitoring can be performed with the naked eye. These data confirmed that the effects observed are general and not specific to the sequence of extra nucleotides added to the RBA.

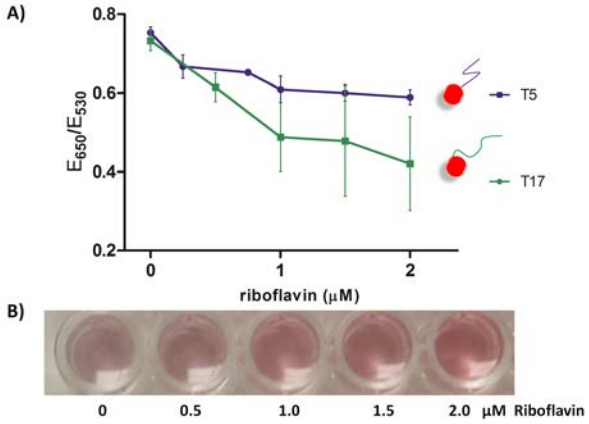


CONCLUSIONS. In this work, we explored the effects of modifications to an aptamer sequence on the colorimetric response of Apt-AuNPs to their target. We used a non-labeled riboflavin binding aptamer and unmodified AuNPs as a model to study the interactions of aptamers and AuNPs. We observed that parameters like ionic strength and aptamer length affected the sensing response. The RBA was chosen to test an aptamer that has not been previously used in combination with AuNPs for colorimetric sensing. The RBA-AuNPs were obtained by simply adsorbing the oligos on the surface of the AuNPs. In the absence of riboflavin, the RBA-AuNPs aggregated when challenged with NaCl. Exposing the RBA-AuNPs to riboflavin improved their stability by preventing their aggregation when challenged with high ionic strength media. This was used to design a colorimetric assay for riboflavin. We observed that addition of extra random nucleotides to the 5'end of the aptamer, that did not interact with the binding sequence, affected the response of the RBA-AuNPs obtained. In particular, it was observed that the aptamer length modified the magnitude of the RBA-AuNPs response to riboflavin. Adding five extra bases to the RBA suppressed part of the response of the Apt-AuNPs to riboflavin, but adding seventeen extra bases produced Apt-AuNPs that responded efficiently to the target; however, their response was not as good as the system obtained with the RBA with no nucleotides added. We studied the cause of the observed effects by UV-Vis spectroscopy and DLS, observing that the response of the Apt-AuNPs was directly correlated to their stability. The RBA-AuNPs stability was affected by the aptamer used, but was not directly correlated to the aptamer length. Importantly, when the extra nucleotides were replaced

by thymine bases, a similar effect was observed, confirming that the results reported were not specific to the sequence of the extra nucleotides used. This work shows that a more profound understanding of the interactions between aptamers and AuNPs is necessary to improve the design of these colorimetric sensing materials. It is important to mention that, based on previous work by our group and others, the effect observed with the RBA may not be necessarily extrapolated to other aptamers. We are currently working with other aptamers to evaluate the effects of similar modifications on their sequences and the Apt-AuNPs' response.

ACKNOWLEDGMENT. This work was funded by the Air Force Office of Scientific Research. Partial funding for this work was provided by the US Criminal Investigation Lab. JLC participation was supported in part by an appointment to the Postgraduate Research Participation Program at the U.S. Air Force Research Laboratory administered by the Oak Ridge Institute for Science and Education through an interagency agreement between the U.S. Department of Energy and USAFRL.

SUPPORTING INFORMATION. Additional information as noted in the text. The material is available free of charge via the internet at http://pubs.acs.org.

**Figure 1.** Typical RBA-AuNPs response to riboflavin. A) UV-Vis scans showing the change in the aggregation state of RBA-AuNPs upon exposure to NaCl. The black line shows the scan when no riboflavin was added to the AuNPs prior to addition of salt. The other scans show the response of the same Apt-AuNPs exposed to increasing riboflavin concentrations before NaCl was added. B) Quantification of the Apt-AuNPs response to riboflavin (red line) and the negative control QCA (blue line). The aggregation state was quantified by the ratio of aggregated to dispersed Apt-AuNPs taken at their extinction at 650 and 530 nm, respectively.

**Figure 2.** A) Comparison of the response of the Apt-AuNPs to riboflavin, the buffer used was the same for NoTail and ShortTail-Apt-AuNPs: 12.5 mM Hepes, 1.25 mM $MgCl_2$. The buffer used for the

LongTail-Apt-AuNPs contained 8.3 mM Hepes and 1 mM $MgCl_2$. The NaCl concentrations added were 261 mM for NoTail-Apt AuNPs, 346 mM for Short Tail-Apt-AuNPs and 353 mM for LongTail-Apt-AuNPs. The data presented was recorded three minutes after NaCl addition. Experiments were performed in triplicate; the error bars show the standard deviation of the replicates. B) Digital images of the NoTail-Apt-AuNPs after exposure to riboflavin (top) and QCA (bottom), the images shown were taken 4 minutes after salt addition.

**Figure 3.** Aggregation kinetics of the RBA-AuNPs exposed to different riboflavin concentrations. NaCl was added to the RBA-AuNPs suspensions after fifteen minutes incubation with riboflavin. A) NoTail-Apt-AuNPs in 12.5 mM Hepes, 1.25 mM $MgCl_2$, NaCl added 261 mM, B) Short Tail-Apt-AuNPs in 12.5 mM Hepes, 1.25 mM $MgCl_2$, NaCl added 346 mM, C) LongTail-Apt-AuNPs in 8.3 mM Hepes and 1 mM $MgCl_2$, NaCl added 353 mM. Experiments were performed in triplicate; the error bars show the standard deviation of the replicates.

**Figure 4.** DLS size distribution data. Changes in the size distribution of each system were followed during the different steps of the preparation of the riboflavin detection assay. Size distribution of: A) RBA-AuNPs in water; B) after addition of buffer containing 12.5 mM Hepes, 1.25 mM $MgCl_2$ ; and C) after addition of riboflavin in buffer. The systems showed aggregation in binding buffer, but an increase in stability was observed upon addition of the target, due to conformational changes of the aptamer upon binding riboflavin.

**Figure 5.** A) Comparison of the response of Apt-AuNPs obtained with aptamers containing poly(thymine) tails of different lengths. Hepes buffer was used in both cases (12.5 mM) supplemented with 1.25 mM $MgCl_2$. The NaCl concentrations added were 347 mM for T17-Apt-AuNPs and 354 for T5-Apt-AuNPs. B) Digital images of the T17-Apt-AuNPs showing the colorimetric response to riboflavin, the image was taken 6 minutes after salt addition.

**Scheme 1.** Schematic representation of the riboflavin detection assay based on unmodified AuNPs and a non-labeled riboflavin binding aptamer. A) Addition of NaCl produced Apt-AuNPs aggregation due to the increase in ionic strength of the media. B) Exposing the Apt-AuNPs to riboflavin prior to the addition of salt increased their stability, preventing their aggregation.

**Table I.** Sequences of the Aptamers Used in this Study

REFERENCES.


1. Rosi, N. L.; Mirkin, C. A. *Chem. Rev*., **2005**, *105*, 1547-1562.

2. Giljohann, D. A.; Seferos, D. S.; Daniel, W. L.; Massich, M. D.; Patel, P. C.; Mirkin, C. A. *Angew. Chem. Int. Ed.* **2010**, *49*, 3280-3294.

3. Iliuk, A. B.; Hu, L.; Tao, W. A. *Anal. Chem.* **2011**, *83*, 4440-4452.

4. Alivasatos, A. P.; Johnsson, K. P.; Peng, X.; Wilson, T. E.; Loweth, C. J.; Bruchez Jr.; M. P., Schultz; P. G. *Nature* **1996,** *382*, 609-611.

5. Elghanian, R.; Storhoff, J. J.; Mucic, R. C.; Letsinger, R. L.; Mirkin C. A. *Science* **1997**, *277*, 1078-1081.

6. Wang, L.; Liu, X.; Hu, X.; Song, S.; Fan, C. *Chem. Commun*. **2006**, 3780-3782.

7. Wei, H.; Li, B.; Li, J.; Wang, E.; Dong, S. 2 *Chem. Commun.* **2007**, 3735-3737.

8. Liu, J.; Lu, Y. *Angew. Chem. Int. Ed.* **2006**, *45*, 90-94.

9. Chávez, J. L.; Lyon, W.; Kelley-Loughnane, N.; Stone, M. O. *Biosens. Bioelectron*. **2010**, *26*, 23-28.

10. Pavlov, V.; Xiao, Y.; Shlyahovsky, B.; Willner I. *J. Am. Chem. Soc.* **2004**, *126*, 11768-11769.

11. Wang, J.; Meng, W.; Zheng, X.; Liu, S.; Li, G. *Biosens. Bioelectron*. **2009**, *24*, 1598-1602.

12. Zhao, W.; Chiuman, W.; Lam, J. C. F.; McManus, S. A.; Chen, W.; Cui, Y.; Pelton, R.; Brook, M. A.; Li, Y. *J. Am. Chem. Soc.* **2008**, *130*, 3610-3618.

13. Chen, S-J.; Huang, Y-F.; Huang, C-C.; Lee, K-H.; Lin, Z-H.; Chang, H-T. *Biosens. Bioelectron*. **2008**, *23*, 1749-1753.

14. Li, H.; Rothberg, L. *PNAS* **2004**, *101*, 14036-14039.

15. Zheng, Y.; Wang, Y.; Yang, X. *Sensors and Actuators B* **2011**, *156*, 95-99.

16. Tuerk, C.; Gold, L. *Science* **1990**, 249, 505-510.

17. Ellington, A. D.; Szostak, J. W. *Nature* **1990**, 346, 818-822.

18. Mannironi, C.; Di Nardo, A.; Fruscoloni, P.; Tocchini-Valentini, G. P. *Biochemistry* **1997**, *36*, 9726-9734.

19. Katilius, E.; Flores, C.; Woodbury, N. W. *Nucleic Acids Research* **2007**, 35, 7626-7635.

20. Ruff, K. M.; Snyder, T.; Liu, D. R. *J. Am. Chem. Soc.* **2010**, *132*, 9453-9464.

21. Liu, J.; Lu, Y. *J. Am. Chem. Soc.* **2007**, *129*, 8634-8643.

22. Collet, J. R.; Cho, E. J.; Ellington, A. D. *Methods* **2005**, *37*, 4-15.

23. Progodich, A. E.; Lee, O-S.; Daniel, W.L.; Seferos, D. S.; Schatz, G. C.; Mirkin, C. A. *J. Am. Chem. Soc.* **2010**, *132*, 10638-10641.

24. Brown, K. A.; Park, S.; Hamad-Schifferli, H. *J. Phys. Chem. C.* **2008**, *112*, 7517-7521.

25. Kimura-Suda, H.; Petrovykh, D. Y.; Tarlov, M. J.; Whitman, L. J. *J. Am. Chem. Soc.* **2003**, *125*, 9014-9015.

26. Storhoff, J. J.; Elghanian, R.; Mirkin, C. A.; Letsinger, R. L. *Langmuir* **2002**, *18*, 6666-6670.

27. Wolf, L. K.; Gao, Y.; Georgiadis, R. M. *Langmuir* **2004**, *20*, 3357-3361.

28. Lauhon, C. T.; Szostak, J. W. *J. Am. Chem. Soc.* **1995**, *117*, 1246-1257.

29. Hagen, J. A.; Kim S. N.; Bayraktaroglu, B.; Leedy, K.; Chávez, J. L.; Kelley-Loughnane, N.; Naik R. R.; Stone, M. O. *Sensors* **2011**, *11*, 6645-6655.

30. Liu, J.; Lu, Y. *Nature Protocols* **2006**, *1*, 246-252.

31. Hackley, V. A., Clogston J. D. **2007**, *Measuring the Size of Nanoparticles in Aqueous Media Using Batch-Mode Dynamic Light Scattering*, NIST - NCL Joint Assay Protocol PCC-1

32. Zuker, M. *Nucleic Acid Res.* **2003**, *31*, 3406-3415.

33. Sandström, P.; Boncheva, M.; Åkerman, B. *Langmuir* **2003**, *19*, 7537-7543.

34. Sapsford, K. E.; Tyner, K. M.; Dair, B. J.; Deschamps, J. R.; Medintz, I. L. *Anal. Chem.* **2011**, *83*, 4453-4488.

35. Zook, J. M., MacCuspie, R. I., Locascio, L. E., Halter, M. D., Elliott, J. T. *Nanotoxicology* **2010**, 1-14.